LIGO Laboratory / LIGO Scientific Collaboration

LIGO-T040106-00-K *Advanced LIGO UK* May 2004

Measurement of LIGO hybrid OSEM sensitivity

Nick Lockerbie

Distribution of this document:
Inform aligo_sus

This is an internal working note
of the Advanced LIGO Project, prepared by members of the UK team.

Institute for Gravitional Research
University of Glasgow

E-mail

Department of
University of Birmingham
Phone
Fax
E-mail:

Engineering Department
CCLRC Rutherford Appleton Laboratory
Chilton, Didcot, Oxon OX12 0NA
Phone +44 (0) 1235 44 5297
Fax +44 (0) 1235 445843

Particle Physics and Astronomy Research Council (PPARC)

http://www.ligo.caltech.edu/

http://www.eng-external.rl.ac.uk/advligo/papers_public/ALUK_Homepage.htm.

UNIVERSITY OF STRATHCLYDE

Measurement of LIGO hybrid OSEM sensitivity

The work reported here was undertaken in order to measure the displacement sensitivity of a LIGO hybrid OSEM. The electromechanical part of the OSEM comprising the feedback coil assembly, an integral infrared emitter/detector shadow sensor pair, and a magnet/Flag assembly, was supplied to Strathclyde from the US via Stuart Aston of Birmingham, together with a circuit diagram of the existing 'Satellite Amplifier' (from Jay Heefner, Caltech). The circuit diagram is LIGO drawing D961289, Rev. B.

Mechanical assembly

In order to carry out the tests firstly two aluminium-alloy 'L'-brackets were machined, one to carry the body of the OSEM, the other to carry the magnet/Flag assembly. This assembly was stood-off from its bracket using a 12.5 mm long cylindrical aluminium alloy spacer. The L-brackets bearing the OSEM's body and the magnet/Flag assembly were then mounted respectively onto micrometer-adjustable XY and X stages, as shown in Fig. 1. By adjusting the position of the X stage the OSEM's Flag could be driven into/withdrawn from the infrared shadow-sensor, this being mounted within the coil-former of the OSEM's body.

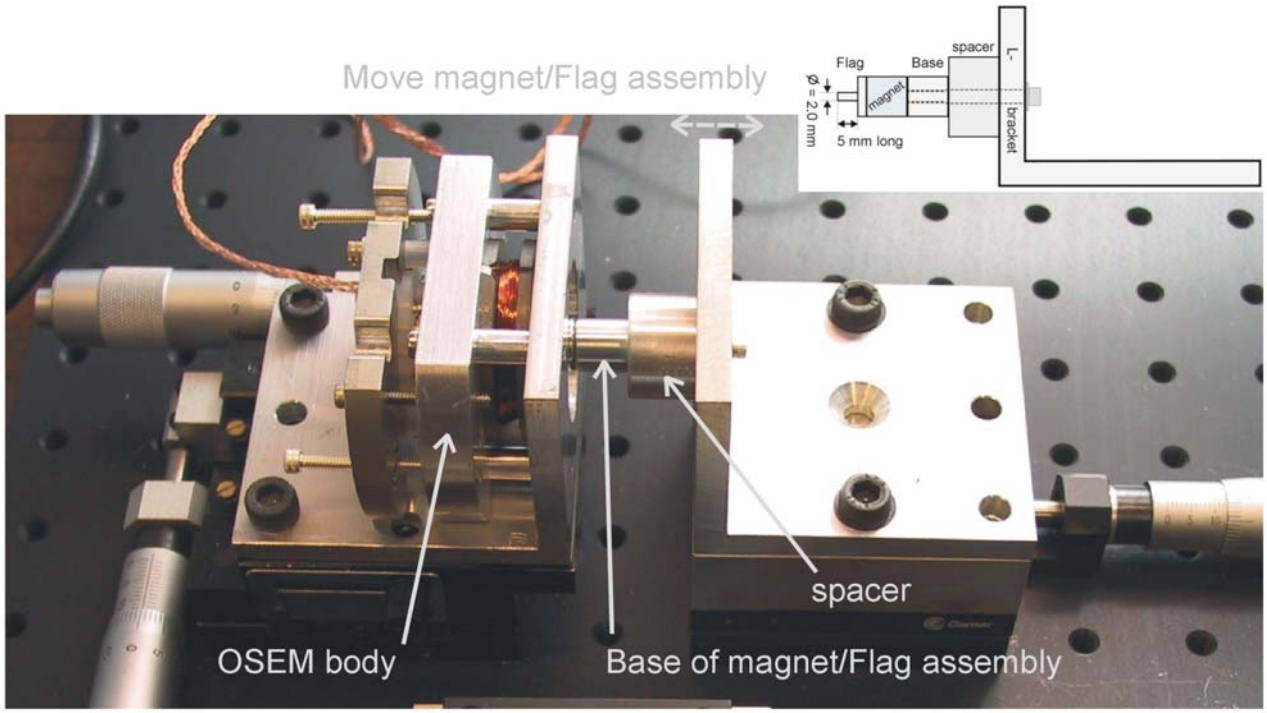

Figure.1 Mechanical test-rig, showing the adjustable XY stage (at Left) and X stage (Right).

OSEM Interface electronics

Secondly, a 'copy' of the Satellite Amplifier electronics was made in order to interface to the shadow sensor, i.e., to supply an appropriate level of constant current to the infrared LED (Honeywell SME2470, an aluminium gallium arsenide device, with an 880 nm peak emission wavelength), and to detect the resulting photocurrent coming from the sensor's matching photodiode detector (Honeywell SMD2420).

The original Satellite Amplifier was designed to work simultaneously with five OSEMs, and so the original circuit was simplified so that it could be used with a single OSEM, whilst retaining the essential features of the original circuit. In consequence dual op-amp ICs (LT1124) were

substituted for the original quad op-amp packages (LT1125). Also, the National Semiconductor LM6321 buffer ICs used in the Satellite Amplifier are now obsolete. A replacement was found in the form of a Burr Brown (TI) BUF634P. Table 1 compares its electrical characteristics with those of the original LM6321. The LM6321 also required protection circuitry in the form of a potential divider comprising two 100k resistors, in order to prevent large voltage differences between its input and output pins—which otherwise might destroy the device. A 100pF feed-forward capacitor was also included with this divider in order to reduce phase-shifts in the buffer. Although these precautions are apparently unnecessary when using the BUF634P, they were retained in the OSEM Interface that was built for this work in order to simulate as closely as possible the noise performance that would have been obtained using the original electronics.

	Gain	slew-rate (V/μs)	Bandwidth (MHz)	Supply current (mA)	Output current (mA)	Input impedance (MΩ)	Supply range (V)
LM6321 (obsolete)	1	800	50	20	±300	5	+5 to ±15
BUF634P	1	2000	30–180 (30 selected)	1.5 (@ 30 MHz)	±250	80 (@ 30 MHz)	+4.5 to ±18

Table 1. Comparison between the original LM6321 and its replacement, the BUF634P.

Inspection of the Satellite Amplifier circuit indicated that it should supply a constant current of 34.8 mA to each infrared LED, rather than the '25 mA' marked on the drawing. Indeed this was found to be the correct value, and so a 34.8 mA LED current has been retained for this work.

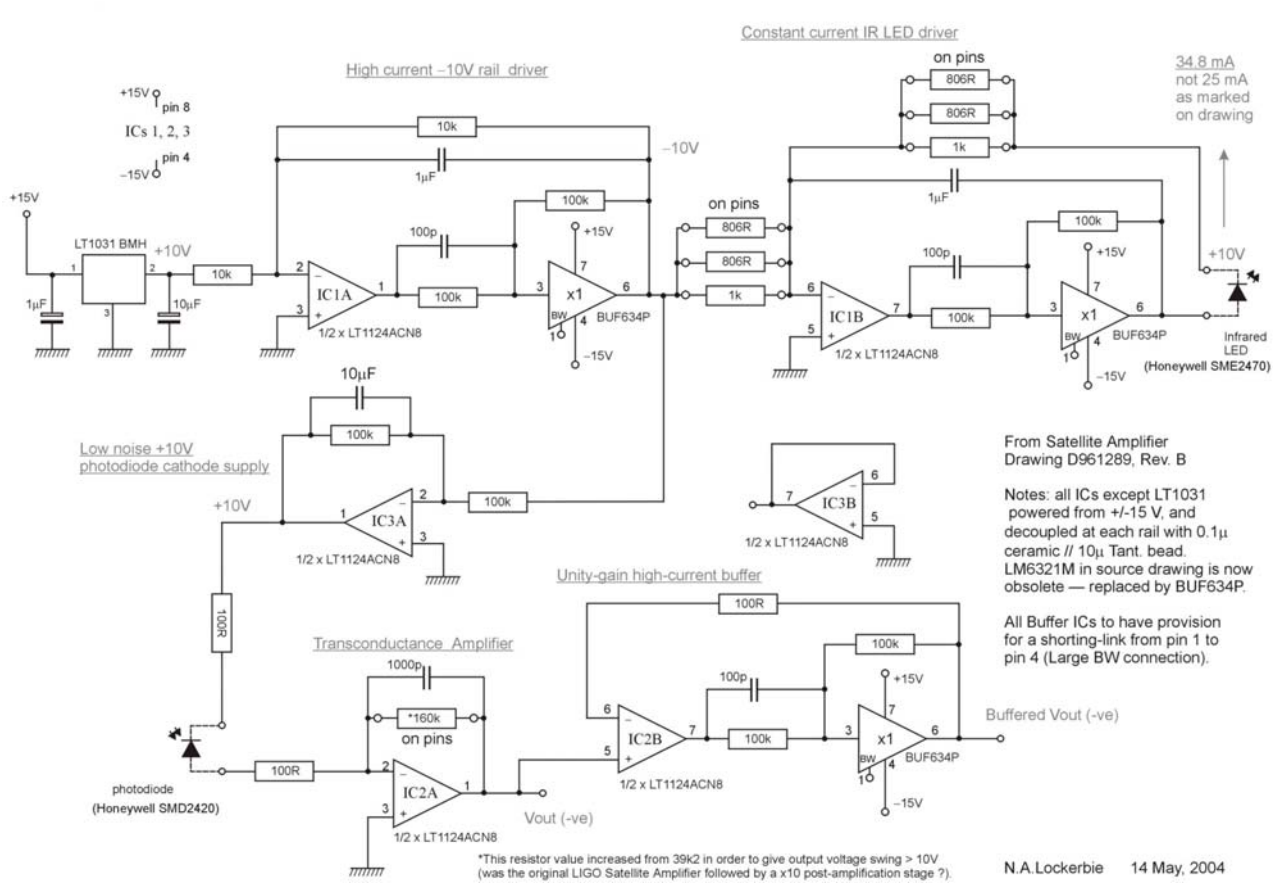

Figure.2 OSEM Interface circuit diagram.

More surprisingly, the transconductance amplifiers' feedback resistors in the Satellite Amplifier were shown as being 39.2k. If the photocurrents were expected to be in the region of 30 μA, which seems to be the case, then the output voltage from each OSEM would have been only of order −1.2 volts (the Satellite Amplifier produces negative outputs with respect to the common line), at the most. Such a voltage seems too low for digitisation purposes, and I expect the Satellite Amplifier outputs to have been followed by x10 (or, even, an offset followed by x20) post-amplifiers.

In this work the transconductance amplifier's feedback resistor was increased in value to 160k, in order to produce an output voltage swing that would be in excess of 10 volts, for the measured photocurrent of 68 μA. The final circuit diagram of the OSEM Interface is shown in Fig. 2.

This Interface circuit was constructed using an overall ground-plane, and it was housed in a steel enclosure, as shown in Fig. 3.

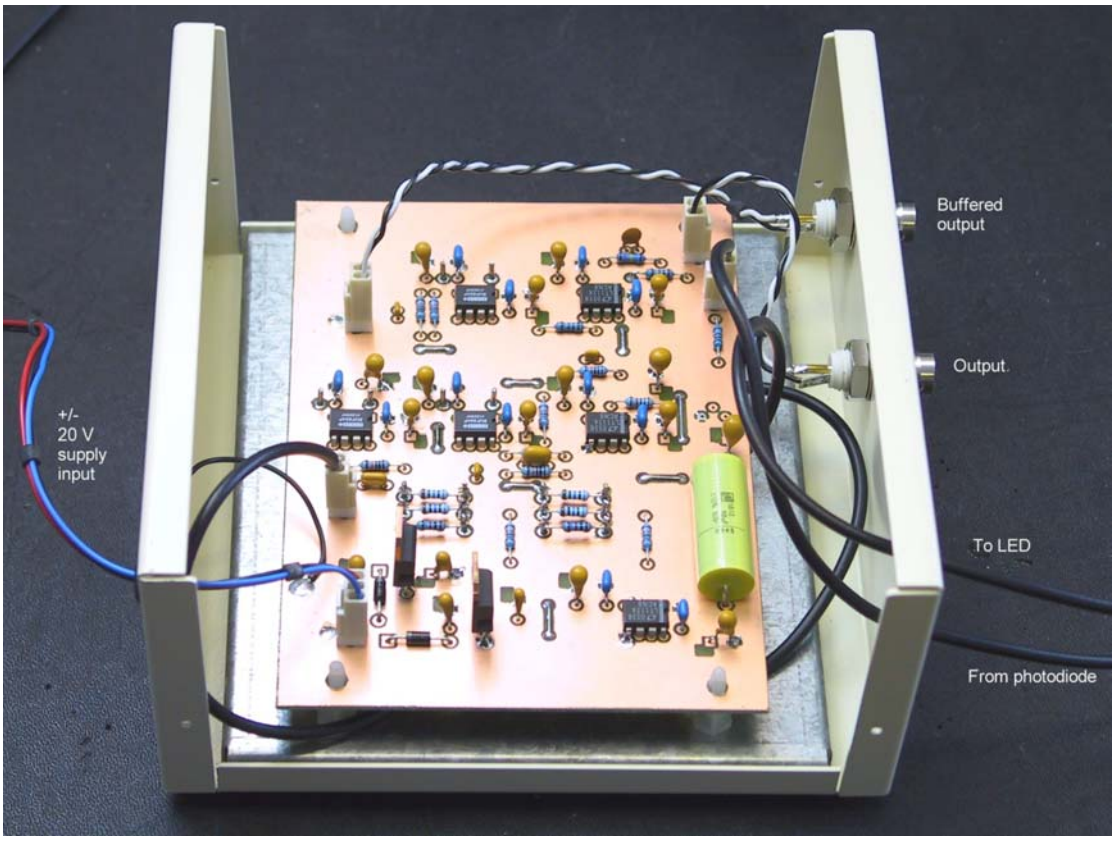

Figure 3. The OSEM Interface just prior to mounting the final component—the LT1031BMH voltage reference IC. Two BNC outputs are shown, the 'Buffered' output being the one used for the displacement sensitivity measurements reported here.

Displacement measurements

The shadow sensor (mounted inside the OSEM's body, shown in Fig. 1) was connected to the OSEM Interface electronics shown in Figs. 2 and 3. The interface electronics was powered from a ±20 V bench PSU, consuming 70 mA (+20 V), and 60 mA (–20 V). The Flag was centralised by eye laterally within the shadow-sensor, using the Y micrometer adjustment for the OSEM body's position.

The position of the Flag within the shadow sensor was adjusted over a range of approximately 4 mm using the X stage (Flag) micrometer adjustment, the buffered output from the Interface electronics being monitored simultaneously. The output voltage was measured using a Fluke 189 multimeter, with 0.1 mV resolution for input voltages below 10 volts. The normal and buffered BNC outputs were found to agree in voltage to better than the resolution of the multimeter.

For the low-frequency noise measurement an AC-coupled SR785 Dynamic Signal Analyzer was connected in parallel with the multimeter, with the Flag's position being adjusted until the DC buffered output read –5.534 volts, i.e. approximately mid-range (photocurrent = 34.6 μA). The ambient temperature during the course of these measurements was relatively high, at 29.2 ºC.

Results 1: Output vs Flag position

With the Flag fully withdrawn the buffered output from the Interface electronics gave a voltage of almost –11 volts (–10.901 V), with the infrared LED of the shadow sensor fully illuminating the photodiode. On the other hand, when the flag was in its fully inserted position the buffered output voltage was close to zero (–34 mV), the Flag now largely masking the LED from the photodiode. The buffered output voltage changed between these two extremes when the Flag was moved over a range of approximately 1 mm, the 'linear' portion of this region being approximately 0.7 mm, as shown in Figure 4. The average slope of the linear region was approximately –15185 $V.m^{-1}$.

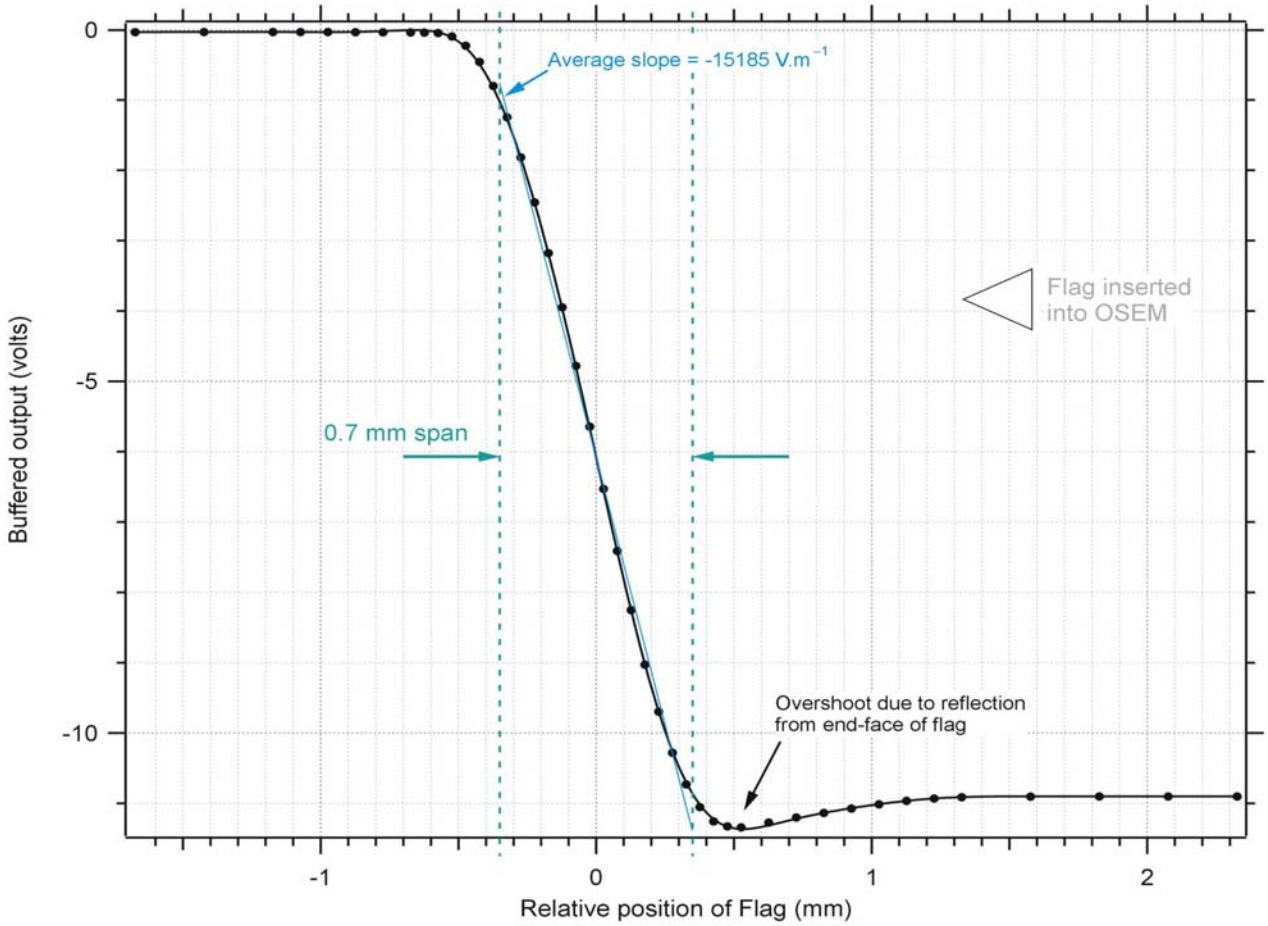

Figure 4. Buffered output voltage as a function of Flag position. The zero of the Flag position scale has been set arbitrarily at the point of the maximum absolute slope.

A small 'overshoot' in signal size (negatively) was seen as the end of the cylindrical Flag approached the detection region of the shadow sensor. This is probably due to reflection from the end-face of the flag temporarily augmenting the infrared coupling between the LED and the photodiode. It may be a useful feature—that could be enhanced.

The noise measurement whose results are reported below was made at a relative Flag position of zero, where the slope sensitivity was at an (absolute) maximum. Subsequently, the OSEM's body was moved transversely by ±0.5 mm about this point, using the Y micrometer adjustment. In other words, the Flag was moved effectively from its axial location either towards the photodiode, or towards the LED. The corresponding change in signal strength was ±7%, showing a fairly good rejection of cross-coupling in the sensor.

An interpolation fit was made to the buffered signal vs Flag position data shown in Fig.4., and this was differentiated in order to produce a differential 'slope sensitivity' for the sensor. The resulting slope sensitivity of the OSEM is shown in Fig.5, the peak absolute value being 17635 $V.m^{-1}$, as indicated in the figure.

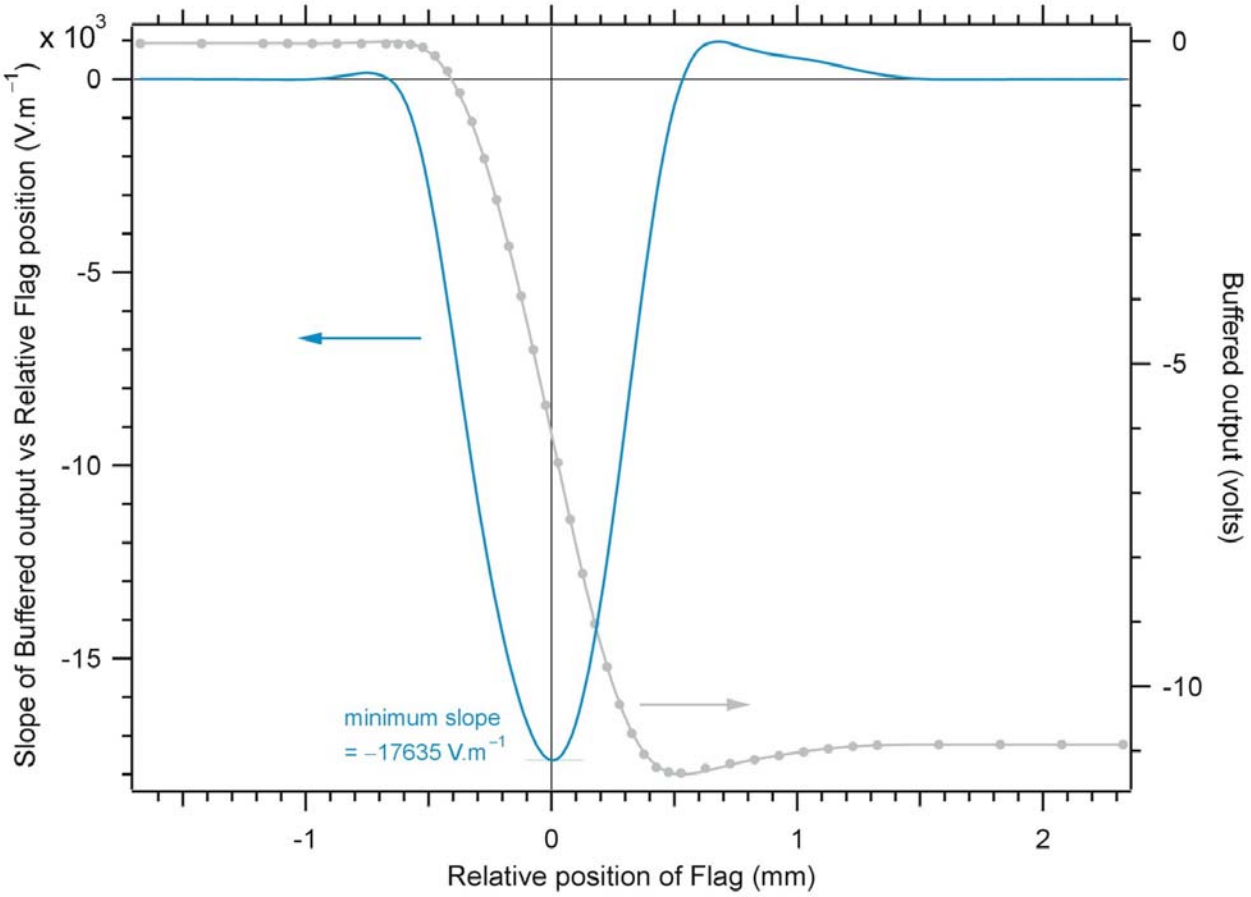

Figure 5. Left ordinate: slope sensitivity of the OSEM's shadow sensor, this being the spatial derivative of a fit to the Right ordinate data: buffered output as a function of Flag position.

Results 2: Noise

The noise measurement for the OSEM was made over a bandwidth of DC–12.5 Hz, at the point of highest slope sensitivity for the device. The resulting spectrum is shown in Fig.6. The noise level at 1 Hz was measured to be –117.183 dBVrms, or 1.38 μV rms/rt-Hz. This figure is approximately 13 dB worse than the noise level at 10 Hz.

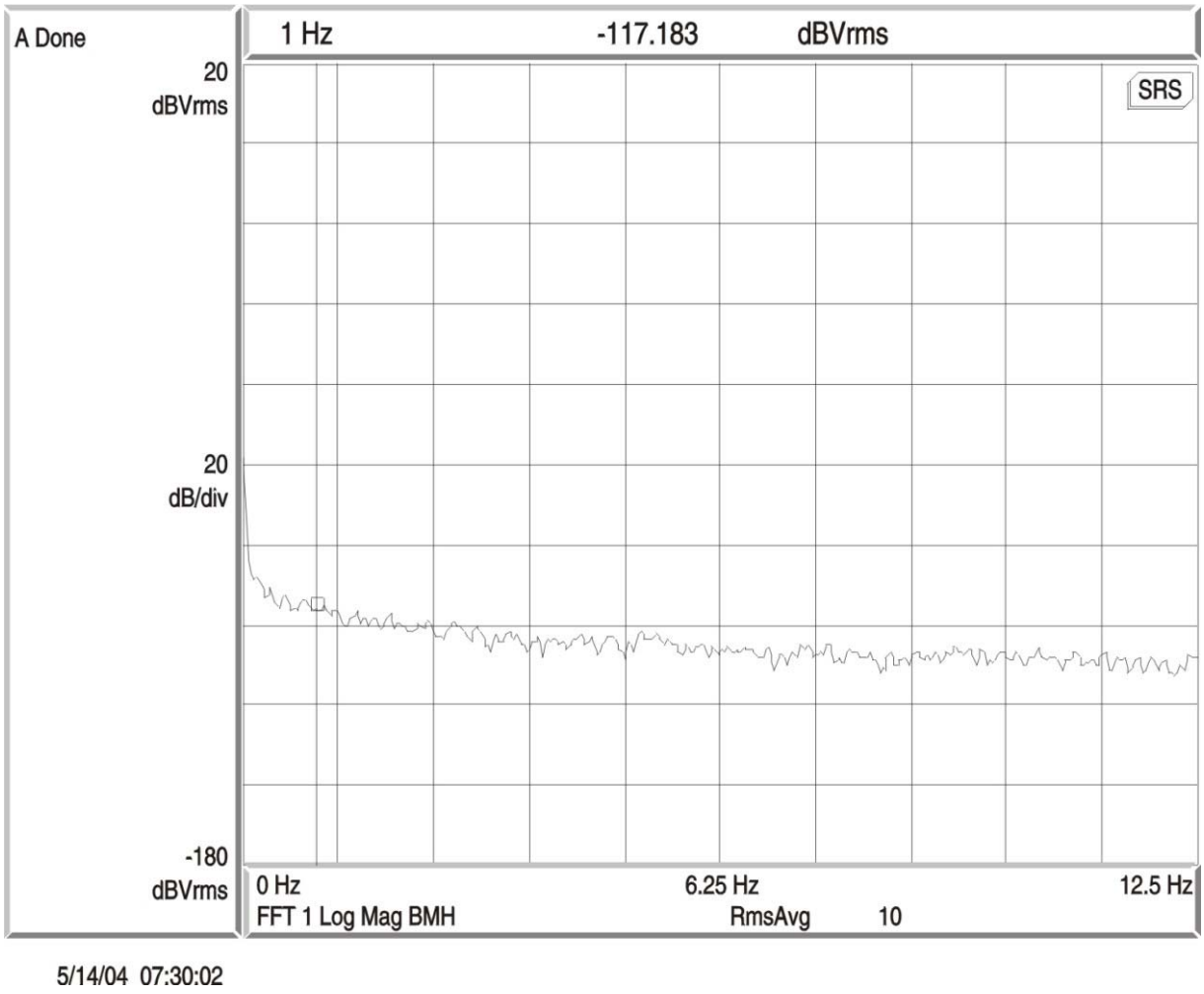

Figure 6. Noise spectrum for the OSEM under test, when connected to the Interface electronics.

Conclusions

The noise measurement at 1 Hz equates to a sensitivity of $(1.38 \times 10^{-6}$ V/rt-Hz)/(15185 V/m), or $\underline{9.1 \times 10^{-11}\ \text{m/rt-Hz}}$, if the average slope sensitivity over the 0.7 mm span of the OSEM is used in conjunction with the noise performance measured at the centre of this range. In a similar way the *peak* in the slope sensitivity, which was found to have a magnitude of 17635 V.m^{-1}, translates into an incremental displacement sensitivity for the OSEM of $\underline{7.8 \times 10^{-11}\ \text{m/rt-Hz}}$, at 1 Hz.

These figures are a factor of 3–4 better than those reported by P. Fritschel and R. Adhikari in the document LIGO-T990089-00, 12 Oct. 1999, where they assessed the same two Honeywell devices, albeit in a lab bench setup, rather than in an actual OSEM. The devices' operating conditions for their work, and for this work, are compared in Table 2.

	Sensing distance (mm)	SME2470 (LED) current (mA)	SMD2420 (PD) Mean photocurrent (μA)	Slope-sensitivity ('sensing-calibration') ($kV.m^{-1}$)	Transconductance amplifier's feedback resistor (kΩ)	Output noise at 1 Hz (μV/rt-Hz)
P. Fritschel and R. Adhikari LIGO-T990089-00	6.35	42	12.5	5.5	100	1.63 (estimated from graph, @ 25 μA)
This work	6.2 (estimated)	34.8	34.6	17.6	160	1.38

Table 2. Comparison between the operating conditions and the measured noise performances of the Honeywell shadow sensor devices used in this work, and in that of P. Fritschel and R. Adhikari, as described in document LIGO-T990089-00.

One factor that stands out from the comparison in Table 2 is the significantly higher current transfer ratio—measured from LED to photodiode—that was recorded in this work. Indeed, the ratio is a factor of 3.3 higher than that found in the LIGO work. Perhaps this detection efficiency factor is largely responsible for the enhanced sensitivity, although the measured noise at 1 Hz was also somewhat lower in this work ?

N.A. Lockerbie
17 May, 2004